Proceedings of the 5th WSEAS/IASME Int. Conf. on SYSTEMS THEORY and SCIENTIFIC COMPUTATION, Malta, September 15-17, 2005 (pp114-119)

Finite Element Analysis of Elastic Transient Ultrasonic Wave Propagation for NDT Applications

G. AIELLO, E. DILETTOSO, N. SALERNO
Dipartimento di Ingegneria Elettrica Elettronica e dei Sistemi
Università degli Studi di Catania
Viale Andrea Doria 6, I-95125 Catania
ITALY
http://wwwelfin.diees.unict.it/

Abstract: - Nondestructive testing techniques are of great relevance nowadays and are extensively employed in almost all areas of engineering to detect defects in products and structures, or to point out deteriorations in industrial plants. The paper deals with techniques which make use of transient ultrasonic waves, the aim being numerical modelling and simulation of their propagation in long cylindrical shell structures affected by axisymmetric defects and/or material inhomogeneities. For this purpose a finite element code has been developed by the authors, who have validated and utilized it to perform simulations, the results of which are presented and discussed.

Key-Words: - **Elastic Wave propagation; Transient; Ultrasounds; Finite Elements; NDT Applications.**

1 Introduction

In the last few decades, ultrasonic nondestructive testing (NDT) techniques have acquired more and more relevance, as is witnessed by the progressive successful widening of their field of application and by the increase in the accuracy and flexibility they offer. Nowadays they are routinely and extensively employed in a great number of different areas of engineering to detect and characterize defects or corrosion phenomena in products and structures, to monitor the degree of safety of critical parts of industrial plants, to evaluate the state of conservation of the historical and artistic heritage, and for many other uses [1], [2], [3], [4].

There is therefore growing interest in developing accurate models to describe the transient propagation of ultrasonic waves through a variety of solid materials and structures which make up the various systems being investigated. Of course, these models then have to be implemented in robust numerical codes, typically finite-element ones, so as to analyse these complex phenomena accurately and efficiently [5], [6].

The aim of this paper is briefly to describe the formulation employed in the finite element code developed by the authors to simulate the propagation of transient ultrasonic waves in elastic linear media, and to present and discuss some preliminary results obtained by using the code; a validation of the code is also given. More specifically, attention is focused on the analysis of thin shell cylindrical structures, which are commonly used to model geometrically long pipes. Because of the presence of defects in the pipes inside which the propagation of ultrasonic waves has to be simulated, and owing to the extremely complex geometries of the real-world structures to be taken into account, it is essential to develop a finite element code able to carry out a fully tri-dimensional analysis which also allows inhomogeneities and/or anisotropies to be treated [7]. The paper is organized as follows. Sections 2 and 3 describe the mathematical and numerical formulation employed to develop the code; in Section 4 a validation of the code is given and some results of the simulations performed are presented and discussed in detail; finally, in Section 5 the authors' conclusions are given.

2 Mathematical Formulation

According to the relevant literature [8], [9], [10], we study the propagation of ultrasonic waves in solids by means of the displacement vector **u.** In an isotropic homogeneous medium, under the standard assumptions of linear elasto-dynamics theory and the absence of viscosity, the governing equation is:

$$(\lambda+\mu)\nabla\nabla\cdot\mathbf{u}+\mu\Delta\mathbf{u}+\mathbf{f}_v=\rho\ddot{\mathbf{u}} \quad , \qquad (1)$$

where $\mathbf{f}_v$ is the body force, λ and μ are the Lamé constants, ρ is the volume mass density and the dots denote the second-order time derivative .

Equation (1) has to be solved in a bounded domain Ω with boundary $\partial\Omega=\partial\Omega_g\cap\partial\Omega_m$ on which an assigned displacement $\mathbf{u}\big|_{\partial\Omega g}=\mathbf{u_g}$ (Dirichlet or geometrical condition) and/or an assigned traction $\mathbf{f}\big|_{\partial\Omega m}=\mathbf{f_m}$ (Newmann type or mechanical boundary condition) have to be imposed on the boundary; the initial conditions $\mathbf{u}_0=\mathbf{u}(P,0)$ $\dot{\mathbf{u}}_0=\dot{\mathbf{u}}(P,0)$ must also be specified in each point P of Ω.

Making use of **u** it is then possible to compute the strain tensor ξ_{ij} i,j=1,2,3 in rectangular Cartesian coordinates as [8]:

$$\xi_{ij}=\frac{1}{2}\left(\frac{\partial\mathbf{u_i}}{\partial\mathbf{x_j}}+\frac{\partial\mathbf{u_j}}{\partial\mathbf{x_i}}\right) \quad . \qquad (2)$$

Equation (1) can be derived by imposing a vanishing first-

order variation $\delta^{(1)}F$ of the following functional F(**u**,t):

$$F(\mathbf{u},t)=\int_{\Omega}\left[-w_e+\left(-\rho\ddot{\mathbf{u}}+\mathbf{f}_v\right)\cdot\mathbf{u}\right]+\int_{\partial\Omega_m}\mathbf{f}_m\cdot\mathbf{u}, \quad (3)$$

where $w_e=\frac{1}{2}\sum_{i,j=1}^{3}\left(\lambda\xi_{ii}\,\xi_{jj}+2\mu\,\xi_{ij}^2\right)$ is the total strain energy of the body [11]. Starting from (3) it is straightforward to write $\delta^{(1)}F$ as:

$$\delta^{(1)}F=\int_{\Omega}\left[-\delta w_e+\left(-\rho\ddot{\mathbf{u}}+\mathbf{f}_v\right)\cdot\delta\mathbf{u}\right]+\int_{\partial\Omega_m}\mathbf{f}_m\cdot\delta\mathbf{u}\,; \quad (4)$$

Note that in deriving (4) the variation $\delta\mathbf{u}(P)$ of **u** has to be considered as time-independent. Then, by means of (2) it is easy to deduce the following expression for δw_e, which will be used in the next section:

$$\delta w_e=\sum_{i,j=1}^{3}\left[\lambda\frac{\partial u_j}{\partial x_j}\frac{\partial\delta u_i}{\partial x_i}+\mu\left(\frac{\partial u_j}{\partial x_i}\frac{\partial\delta u_j}{\partial x_i}+\frac{\partial u_j}{\partial x_i}\frac{\partial\delta u_i}{\partial x_j}\right)\right]. \quad (5)$$

In fact, as

$$\delta w_e=\sum_{i,j=1}^{3}\left(\lambda\xi_{jj}\,\delta\xi_{ii}+2\,\mu\xi_{ij}\,\delta\xi_{ij}\right), \quad (6)$$

and

$$\xi_{jj}\,\delta\xi_{ii}=\frac{\partial u_j}{\partial x_j}\frac{\partial\delta u_i}{\partial x_i} \quad (7a)$$

$$\sum_{i,j=1}^{3}\xi_{ij}\,\delta\xi_{ij}=\frac{1}{2}\sum_{i,j=1}^{3}\left(\frac{\partial u_j}{\partial x_i}\frac{\partial\delta u_j}{\partial x_i}+\frac{\partial u_j}{\partial x_i}\frac{\partial\delta u_i}{\partial x_j}\right), \quad (7b)$$

through some algebraic manipulations expression (6) is deduced. Of course, making use of standard calculus tools, expression (4) can be recast in such a way as to prove that the stationary of (4) occurs when the solution of the boundary/initial value problem (1) is considered [11].

3 Numerical Formulation

In order to solve the boundary/initial value problem (1) numerically, we adopt a finite-element semi-discretization procedure in which the Raylegh-Ritz variational method is employed to discretize the problem spatially with respect to the Cartesian coordinates x_1, x_2 and x_3, whereas a direct integration method is used to carry out the time-history analysis [12], [13]. Making use of this approach, a system of linear second-order coupled differential equations of the form:

$$\mathbf{M}\ddot{\mathbf{u}}_n+\mathbf{K}\mathbf{u}_n=\mathbf{R}_n \quad (8)$$

is derived, where $\mathbf{u}_n=\mathbf{u}(n\Delta t)$ and $\ddot{\mathbf{u}}_n=\ddot{\mathbf{u}}(n\Delta t)$ are the vectors containing the (unknown) nodal values of the displacement vector **u** and of the acceleration vector $\ddot{\mathbf{u}}$, respectively; **M** and **K** are two square matrices, the former called the consistent mass matrix and the latter the stiffness matrix; $\mathbf{R}_n$ is the vector of known terms, its entries coming from both the boundary/initial conditions and the body (weight) force (however, in the present case, the contributions to $\mathbf{R}_n$ arising from the body force and the mechanical boundary conditions were discarded, as the influence of the former is quite negligible in the current context, and the latter does not concern the analysis being performed; in our formulation, therefore, $\mathbf{R}_n$ is only due to the inhomogeneous Dirichlet boundary/initial conditions and it is built by rearranging the known terms in the space-discretized equations by the standard per-element FEM assembly procedure); the integer n specifies the number of time iterations; and, finally, Δt is the size of the time step of the time integration scheme adopted, details of which will be given below.

Let us now consider the criteria we adopted to number the equations and the unknowns of (9). Since the cardinality of the vectors, as well as the order of the matrices present in (9) is 3N, N being the number of nodes in the finite-element mesh with unknown displacement, each index h of a row in these arrays and each index k of a column (if any) can be written as h=3(p-1) +i and k=3(q-1) +j, where p and q specify a pair of nodes and i and j a pair of components, respectively: for example, the entry $(\mathbf{M})_{hk}$ stands for the coefficient of the j-th component of the (unknown) displacement vector at the node q in the equation of the i-th component of the (unknown) displacement vector at node p.

As regards the expression of the entries of **M** and **K**, the first step in order to derive them is to expand the components of **u,** $\ddot{\mathbf{u}}$ and $\delta\mathbf{u}$ in terms of scalar shape functions α_p:

$$u_j=\sum_{q=1}^{N'}(\mathbf{u})_k\,\alpha_q \quad (9a) \qquad \ddot{u}_j=\sum_{q=1}^{N'}(\ddot{\mathbf{u}})_k\,\alpha_q \quad (9b)$$

$$\delta u_i=\sum_{p=1}^{N'}(\delta\mathbf{u})_h\,\alpha_p \quad (9c) \qquad \delta u_j=\sum_{p=1}^{N'}(\delta\mathbf{u})_l\,\alpha_p\,, \quad (9d)$$

N' being the total number of nodes and l=3(p-1)+j, and then to introduce the expansions (9a), (9c) and (9d) into expression (5). However, in this way, in the fourfold sum over the indices i, j, p and q thus obtained both $(\delta\mathbf{U})_h$ and $(\delta\mathbf{U})_l$ appear. In order to transform it in such a way that only $(\delta\mathbf{U})_h$ appears, in the part of this sum containing $(\delta\mathbf{U})_l$, which comes from the expansion of the first term on the right-hand side of (7b), it is necessary to exchange the indices $i\rightarrow j$ and $j\rightarrow i$; in fact, by so doing the index l transforms to h, and $(\delta\mathbf{U})_l$ becomes $(\delta\mathbf{U})_h$; note that by this exchange the index k takes the new value m=3(q-1)+i and thus some terms containing $(\mathbf{U})_m$ appear in the sum. After this, the following expression is deduced:

$$\delta w_e = \sum_{i=1}^{3}\sum_{p=1}^{N'}\left[\sum_{j=1}^{3}\sum_{q=1}^{N'}\left(\lambda\frac{\partial\alpha_p}{\partial x_i}\frac{\partial\alpha_q}{\partial x_j}+\mu\frac{\partial\alpha_p}{\partial x_j}\frac{\partial\alpha_q}{\partial x_i}\right)(\mathbf{U})_k\right](\delta\mathbf{U})_h$$

$$+\sum_{i=1}^{3}\sum_{p=1}^{N'}\left[\mu\sum_{q=1}^{N'}(\mathbf{U})_m\nabla\alpha_p\cdot\nabla\alpha_q\right](\delta\mathbf{U})_h \qquad (10).$$

By imposing the stationary of functional (4) and taking into account the arbitrariness of $(\boldsymbol{\delta}\mathbf{U})_h$, one deduces from inspection of (10) an expression for the entries of **K**:

$$(\mathbf{K})_{hk} = \begin{cases} \int_\Omega\left[(\lambda+\mu)\frac{\partial\alpha_p}{\partial x_i}\frac{\partial\alpha_q}{\partial x_j}+\mu\nabla\alpha_p\cdot\nabla\alpha_q\right] & i=j \\ \int_\Omega\left(\lambda\frac{\partial\alpha_p}{\partial x_j}\frac{\partial\alpha_q}{\partial x_i}+\mu\frac{\partial\alpha_p}{\partial x_i}\frac{\partial\alpha_q}{\partial x_j}\right) & i\neq j \end{cases} \qquad (11)$$

In a similar way, discretizing the dynamic term -ρ**ü** in (4) by means of the expansion (9b), the expression for **M** is deduced:

$$(\mathbf{M})_{hk} = \int_\Omega \rho\,\alpha_p\,\alpha_q \quad i=j,\ (\mathbf{M})_{hk}=0\ i\neq j \quad ; \qquad (12)$$

note that in the last two expressions the nodes p and q have be considered as belonging to the same finite element; moreover, by inspection it results from (11) and (12) that the matrices **K** and **M** are both symmetric.

In the literature there are a number of methods to carry out the time integration of equation (8), and after careful examination we decided to use the standard central-difference method, for two main reasons [12]. Firstly, in the absence of dissipative effects, leading to the appearance of a first-order time derivative term in equation (8), and thus of a damping matrix, the method can be made explicit by diagonalizing the consistent mass matrix **M** by means of an effective and accurate lumping scheme, such as the HRZ one [12]; in this way, the disadvantage of the method being conditionally stable, thus requiring a sufficiently small time step to guarantee the numerical stability of the procedure, is widely compensated for by the conspicuous decrease in the computational effort needed to compute **u**, since it is no longer necessary in such a case to solve a linear algebraic system of a high order at each time iteration step. Secondly, the method is robust, second-order accurate and easy to implement.

Applying the central-difference method to equation (8), the following linear algebraic system is obtained [12]

$$\mathbf{M}\,\mathbf{u}_{n+1} = (\Delta t)^2\mathbf{R}_n - (\Delta t)^2\mathbf{K}\mathbf{u}_n + \mathbf{M}(2\mathbf{u}_n - \mathbf{u}_{n-1}) \quad (13);$$

then, making use of the HRZ mass lumping technique, a diagonal matrix **M'** is derived; its entries are computed by scaling those of **M** lying on its main diagonal by means of a per-element algorithm which preserves the global mass of the element [12]. After this, substituting **M** with **M**' in (14), and solving with respect to $\mathbf{u}_{n+1}$, the following relationship is deduced:

$$\mathbf{u}_{n+1} = (\Delta t)^2(\mathbf{M}')^{-1}\mathbf{R}_n - (\Delta t)^2(\mathbf{M}')^{-1}\mathbf{K}\mathbf{u}_n + (2\mathbf{u}_n - \mathbf{u}_{n-1}) \quad (14)$$

which was employed to compute iteratively $\mathbf{u}_{n+1}$. However, the computation of $\mathbf{u}_1$ from (14) requires knowledge of the starting value $\mathbf{u}_{-1}$ which is related to the initial values $\mathbf{u}_0$, $\dot{\mathbf{u}}_0$ and $\ddot{\mathbf{u}}_0$ by the following second-order approximate power series expansion

$$\mathbf{u}_{-1} = \mathbf{u}_0 - (\Delta t)\dot{\mathbf{u}}_0 + \frac{1}{2}(\Delta t)^2\ddot{\mathbf{u}}_0 \qquad (15)$$

By assuming $\mathbf{u}_0$=0 and $\mathbf{R}_0$=0 it results from (8) that $\ddot{\mathbf{u}}_0$ is zero, so that having assigned $\dot{\mathbf{u}}_0$=0 in our computations, it follows that $\mathbf{u}_{-1}$ is also zero; as a consequence of this, $\mathbf{u}_1$ vanishes.

The stability of the central-difference method requires the following inequality to hold:

$$\Delta t \le \frac{2}{\omega_{\max}} \qquad (16)$$

where ω_{max} is the highest natural frequency of the equation det(**K**-ω^2**M'**)=0. In order to avoid the drawback of the great effort required by the direct numerical computation of ω_{max}, it is common to evaluate an upper bound by making use of Gerschgori's theorem [12] which, for lumped mass matrices **M'**, states that:

$$\omega^2_{\max} \le \max\left(k_{ii} + \sum_{j=1,\,j\neq i}^{n_e}\left|k_{ij}\right|\right) \backslash\, m'_{ii} \qquad (17)$$

where i=1, 2, …, n_e, and n_e is the number of degrees of freedom per element.

4 Description of the Results

On the basis of the formulations described in the previous sections we worked out an FEM code for analysis of the propagation of transient ultrasonic waves in elastic structures. Actually, this code is only a module of the much larger and more powerful FEM research code ELFIN, which has been developed by the authors and their colleagues at the University of Catania over the last twenty years, for the computation of electromagnetic fields in almost all areas of electrical engineering [14].

In order to validate our code, it was decided to compare the results obtained by means of ELFIN with analogous ones derived by making use of the commercial FEM code ANSYS.

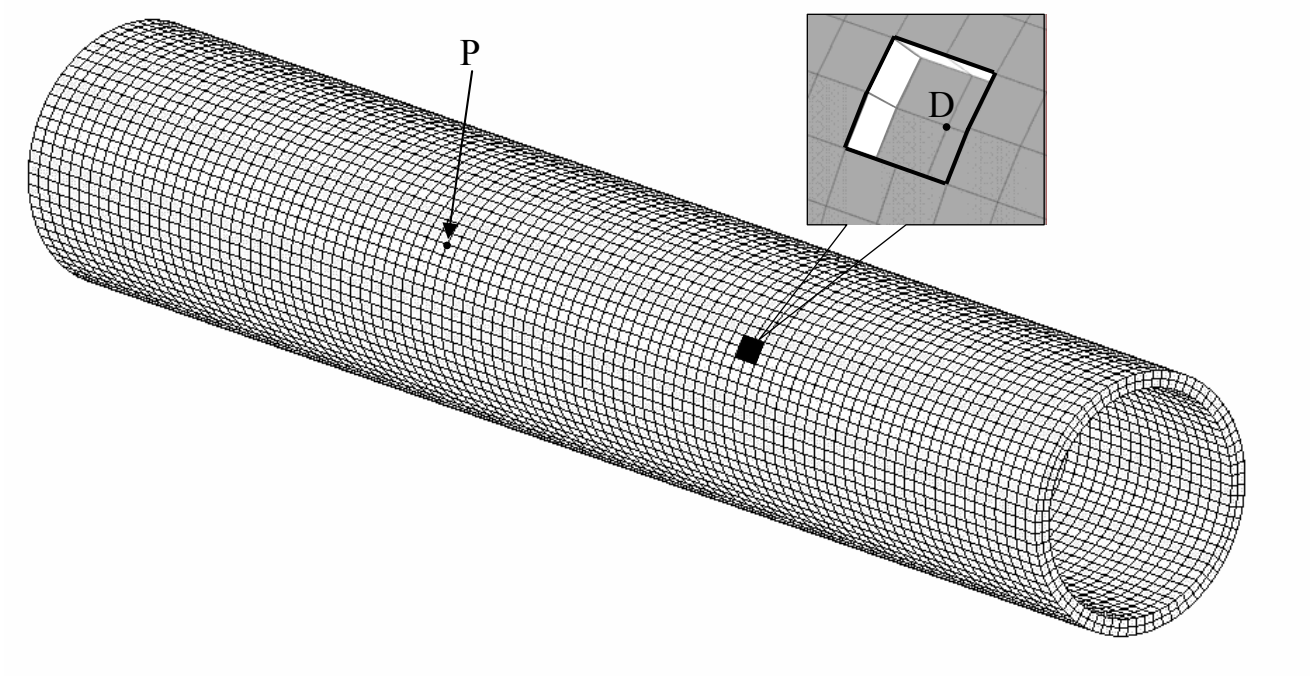

FIG. 1 – FINITE ELEMENT MESH, DEFECT AND OBSERVATION POINT P.

The structure taken into consideration was a pipe modelled geometrically as a homogeneous hollow cylinder with thickness t=5,5 mm, outer radius r_o and inner radius r_i of 43,0 mm and 37,5 mm respectively, and length l=500,0 mm; the material was steel of type 715 whose parameters of interest have the following values: modulus of elasticity E = 215,80 GN/m^2, Poisson's ratio ν = 0,30 and volume density ρ = 7847,09 kg·/m^3; for the sake of completeness, the values of Lame's constant λ and μ are also given: λ = 124,50 GN/m^2 and μ = 83,00 GN/m^2.

A defect was introduced into this structure, consisting of a rectangular shaped notch. It was centred at point D with polar coordinates (42,05 mm, 180°, 350,00 mm) with respect to the right-hand side cylindrical reference frame, with the origin in the centre of an end of the pipe and the z-axis directed inwards. As regards the notch size, it extends outwards in the radial direction for half of the pipe's thickness, that is to say by 2,75 mm, in the axial one by 10,0 mm, and in the circumferential direction it covers an extension of 10° (see Figure 1).

In the computations performed by means of the ELFIN code the structure was discretized by a regular first-order tetrahedral mesh; the number of subdivisions along the radial, axial and circumferential direction is 2, 100 and 72 respectively, which guarantees an adequate spatial resolution. The presence of the defect was modelled by deleting the finite elements inside the notch; in this way the mesh contains 21.815 nodes and 71.980 finite elements.

On the surface of the pipe a vanishing mechanical boundary condition was imposed everywhere, except for the 72 nodes belonging to the external circumference lying on the plane z=0, where a Dirichlet boundary condition, modeling the action exerted by the piezoelectric transmitter on the pipe, was applied: so the global number of degrees of freedom was 65.229. This action was taken into account by imposing an identical displacement vector on each of these nodes, having only the circumferential component other than zero; the time dependence of this component was a sinusoidal signal modulated in amplitude by a Hanning window of six oscillations with the following waveform:

$$f(t) = A\sin(2\pi ft)\cdot\sin^2(2\pi ft/2n)\ \ 0\le t\le t_0 \qquad (18)$$

where the amplitude A is 1 mm, the modulation frequency f is 55 kHz and the integer n is 6. The overall duration of the signal t_0 is 109,1 μs; outside this time interval the waveform is assumed to be identically zero.

The above boundary/initial conditions were chosen because in an infinite-length thin shell cylinder they would only generate the torsional mode, denoted in the literature as T(0,1), which propagates in a non-dispersive way with a velocity of 3,250 km/s [9], [15].

As regards the simulations performed by means of the ANSYS code, the discretization employed was exactly the same as that just described, except for the finite elements adopted, which were eight-node bricks.

A crucial parameter of the simulations was the minimal time step required by the stability of the explicit numerical integration scheme. The upper bound of the time step computed according to (16) was 228 ns. The analyses were performed taking into consideration an overall duration of 300 μs.

Figure 2 gives the values versus time of the circumferential component of the displacement vector obtained by ELFIN at a point P having coordinates (43,00

mm, 180°, 200,00 mm) in the absence of the defect. In this figure, the wave generated by the transmitter (direct wave), followed after 78 ns by another wave of identical amplitude produced by the reflection of the direct wave by the opposite end of the pipe, is clearly recognizable; it is worth noticing that, as expected, the amplitude of the reflected wave is identical to that of the transmitted one owing to the lack of dissipative phenomena in the model.

Moreover, although it is not graphically shown, the numerical computations confirmed that the other two components, the radial and the axial ones, are several orders of magnitude less than the circumferential one, so they are quite negligible. The wave propagates at a velocity of about 3,150 km/s, which is in good agreement with the evaluated velocity [9].

Figure 3 shows the circumferential component of the displacement vector at point P versus time in the presence of the defect: the dotted line refers to the analysis carried out by means of the ANSYS code, whereas the continuous line refers to that performed by means of the ELFIN code.

By inspection of Figure 3, it is quite evident that the two simulations are in excellent agreement with each other, so it can reasonably be stated that ELFIN was successfully validated.

Moreover, the most relevant difference with respect to the results obtained in the previous analysis consists of the presence of a third wave, between the direct and the reflected wave, originated by reflection from the defect and having a reduced amplitude with respect to the other two: this difference may be a promising starting point in order to identify defects.

5 Conclusions

In the paper we have presented the results of numerical computations carried out by means of a module of the large FEM research code ELFIN, specifically developed by the authors to analyze the propagation of ultrasonic waves in solid elastic media in the context of the NDT technique. The code has been validated and its results discussed in detail. In the near future we intend to make changes to the code so as to reduce considerably the computation time currently required.

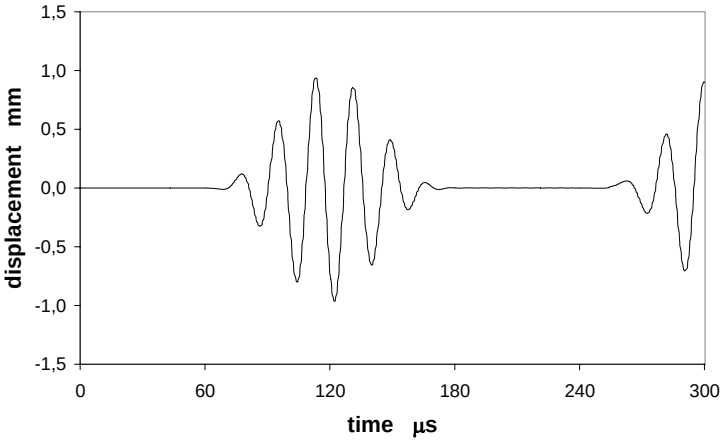

FIG. 2 - CIRCUMFERENTIAL COMPONENT OF THE DISPLACEMENT VECTOR AT POINT P IN ABSENCE OF DEFECT

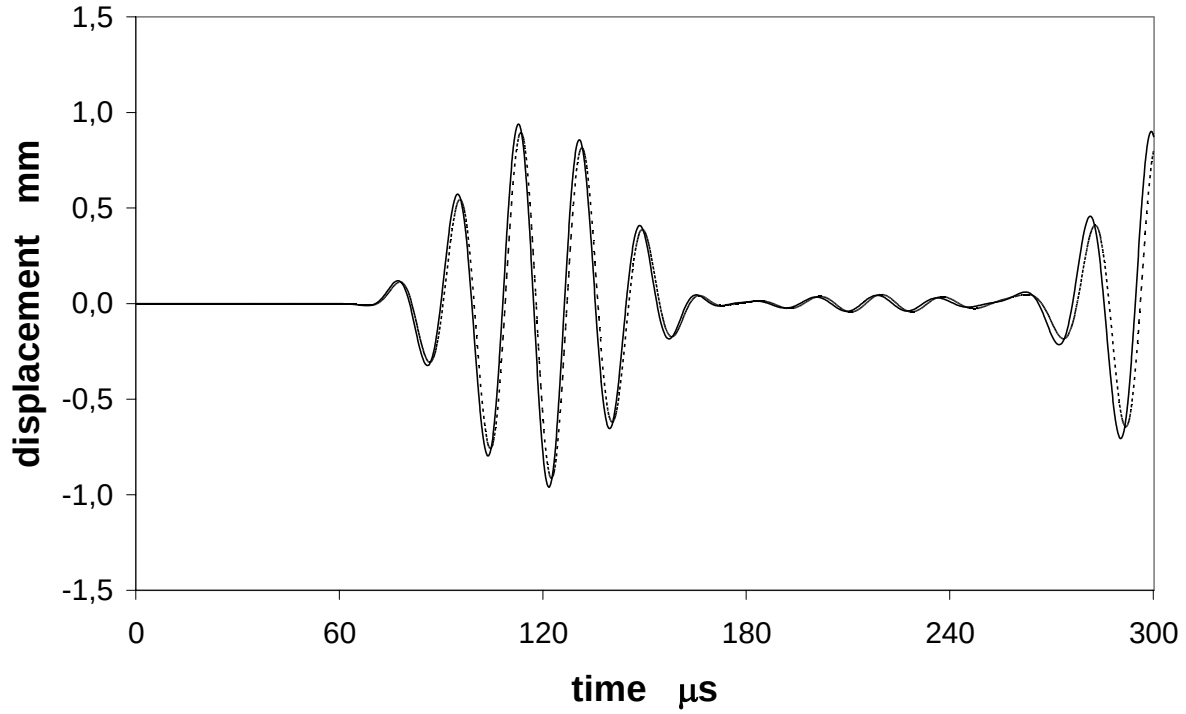

FIG. 3 - CIRCUMFERENTIAL COMPONENT OF THE DISPLACEMENT VECTOR AT POINT P IN PRESENCE OF DEFECT: ANSYS DOTTED LINE, ELFIN CONTINUOUS LINE.

References:

[1] P. Cawley, D. N. Alleyne, The Use of Lamb Wave for Long Range Inspection of Large Structures, *Ultrasonic*, Vol. 34, 1996, pp. 287-290.

[2] D. N. Alleyne, P. Cawley, Long Range Propagation of Lamb Waves in Chemical Plant Pipework, *Material Evaluation*, April 1997.

[3] J. L. Rose, J. Barshinger, Using Ultrasonic Guided Wave Mode Cutoff for Corrosion Detection and Classification, *1998 IEEE Ultrasonic Symposium*, pp. 851-854.

[4] J. Pei, M. I. Yousuf, F. L. Degertekin, B. V. Honein and B. T. Khuri-Yakub, Lamb Wave Tomography and Its Application in Pipe Erosion/Corrosion Monitoring, *1995 IEEE Ultrasonic Symposium,* pp. 795-798.

[5] R. Ludwig, W. Lord, A Finite-Element Formulation for thr Study of Ultrasonic NDT Systems, *IEEE Transaction on Ultrasonic, Ferroelectric and Frequency Control*, Vol. 35, No. 6, 1988, pp. 809-819.

[6] Z. You, M. Lusk, R. Ludwig, W. Lord, Numerical Simulation of Ultrasonic Wave Propagation in Anisotropic and Attenuative Solid Materials, *IEEE Transaction on Ultrasonic, Ferroelectric and Frequency Control*, Vol. 38, No. 5, 1991, pp. 436-445.

[7] D. N. Alleyne, P. Cawley, The Interaction of Lamb Waves with Defects, *IEEE Transaction on Ultrasonic, Ferroelectric and Frequency Control*, Vol. 39, No. 3, 1992.

[8] Y. C. Fung, *Solid Mechanics*, Prentice-Hill, 1965.

[9] K. F. Graff, *Wave Motion in Elastic Solids*, Dover Publications, 1991.

[10] H. Kolsky, *Stress Waves in Solids*, Dover Publications, 1963.

[11] K. Washizu, *Variational Methods in Elasticity and Plasticity*, Pergamon Press, 1972.

[12] R. D. Cook, D. S. Malkus, M. E. Plesha, *Concepts and Applications of Finite Element Analysis*, Prentice-Hill, 1988.

[13] K. J. Bathe, E. L. Wilson, *Numerical Methods in Finite Element Analysis*, , Prentice-Hall, 1976.

[14] G. Aiello, S. Alfonzetti, G. Borzì, N. Salerno, "An Overview of the ELFIN Code for Finite Element Research in Electrical Engineering", *Software for Electrical Engineering: Analysis and Design VI* , A. Konrad e C. Brebbia (Ed), WIT Press, Southampton (Regno Unito), 1999, pp. 143-152.

[15] A. Demma, P. Cawley, M. Lowe, The Reflection of the Fundamental Torsional Mode from Cracks and Notchs in Pipes, *Journal of Acoustical Society of America*, Vol. 114,, n. 2, August 2003.